Towards Accurate Description of Chemical Reaction Energetics by Using Variational Quantum Eigensolver: A Case Study of the C_{2v} Quasi-Reaction Pathway of Beryllium Insertion to H_2 Molecule

Kenji Sugisaki,*[1,2,3] Takumi Kato,[4] Yuichiro Minato,[4] Koji Okuwaki,[5] and Yuji Mochizuki[5,6]

[1]*Department of Chemistry, Graduate School of Science, Osaka City University, 3-3-138 Sugimoto, Sumiyoshi-ku, Osaka 558-8585, Japan.*

[2]*JST PRESTO, 4-1-8 Honcho, Kawaguchi, Saitama 332-0012, Japan.*

[3]*Centre for Quantum Engineering, Research and Education (CQuERE), TCG Centres for Research and Education in Science and Technology (TCG-CREST), 16th Floor, Omega, BIPL Building, Blocks EP & GP, Sector V, Salt Lake, Kolkata 700091, India.*

[4]*Blueqat Inc. 2-40-14 Hongo, Bunkyo-ku, Tokyo 113-0033, Japan.*

[5]*Department of Chemistry, Faculty of Science, Rikkyo University, 3-34-1 Nishi-ikebukuro, Toshima-ku, Tokyo 171-8501, Japan.*

[6]*Institute of Industrial Science, The University of Tokyo, 4-6-1 Komaba, Meguro-ku, Tokyo 153-8505, Japan.*

* Corresponding author: sugisaki@osaka-cu.ac.jp

Abstract

Variational quantum eigensolver (VQE)-based quantum chemical calculations of atoms and molecules have been extensively studied as a computational model using noisy intermediate-scale quantum devices. VQE uses a parametrized quantum circuit defined through an "ansatz" to generate the approximated wave functions, and thus appropriate choice of an ansatz is the most important step. Because most of chemistry problems focus on the energy difference between two electronic states or structures, calculating the total energies in different molecular structures with the same accuracy is essential to correctly understand chemistry and chemical processes. Here we applied numerical simulations of VQE to the quasi-reaction pathway of Be insertion to H_2 molecule, which is the representative systems of both dynamical and static electron correlation effects are prominent. Our numerical simulations revealed that the energy calculated using the conventional unitary coupled cluster (UCC) ansatz exhibits large discrepancy from the full-configuration interaction (CI) value around the point where an avoided crossing occurs. We demonstrated that the multireference unitary coupled cluster with partially generalized singles and doubles (MR-UCCpGSD) ansatz can give more reliable results in respect of total energy and the overlap with the full-CI solution, insisting importance of multiconfigurational treatments in the calculations of strongly correlated systems.

Keywords: Quantum computer | Quantum chemical calculation | Chemical reaction | Electronic structure

1. Introduction

Quantum computers have emerged as one the most disruptive technologies in current science. Computational costs on classical computers of certain problems like prime factorization and group isomorphism grows exponentially against the problem size, but it can be solved in polynomial time by using quantum computers.[1,2] Quantum computers use a quantum bit (qubit) as the minimum unit of information, which can be in arbitrary superposition of $|0\rangle$ and $|1\rangle$ states as in eq (1), where $|0\rangle$ and $|1\rangle$ represent the basis of the quantum states in the Dirac's bra-ket notation, while classical bits can have only one of two values, either 0 or 1.[3] Quantum superpositions and entangled quantum states are the sources of computational powers of quantum computers.

$$|\varphi\rangle = c_0|0\rangle + c_1|1\rangle \doteq \begin{pmatrix} c_0 \\ c_1 \end{pmatrix} \quad (1)$$

Among the diverse topics in quantum computing and quantum information processing, sophisticated quantum chemical calculations of atoms and molecules are one of the most intensively studied realms as the near future applications of quantum computers. In 2005, Aspuru-Guzik and coworkers proposed a quantum algorithm for full-configuration interaction (CI) calculation that gives variationally best possible wave function within the space spanned by the basis set being used, by utilizing a quantum phase estimation (QPE) algorithm.[4] Proof-of-principle experiments of the full-CI calculations of H_2 molecule with the minimal (STO-3G) basis[5] were reported in 2010 by using photonic[6] and NMR[7] quantum processors. Since then, great number of theoretical and experimental studies on the quantum chemical calculations on quantum computer have been reported. QPE-based full-CI is very powerful and exponential speedup against classical counterpart is guaranteed, but the quantum circuit for QPE-based full-CI is so deep that it is quite difficult to obtain meaningful results unless quantum error correction code is implemented and fault-tolerant quantum computing is realized.

A quantum–classical hybrid algorithm known as a variational quantum eigensolver (VQE) was proposed in 2014[8,9] as the alternative computational model in the noisy intermediate-scale quantum (NISQ)[10] era. VQE uses a quantum processing unit (QPU) for the preparation of approximated wave function by utilizing parameterized quantum circuits and evaluation of energy expectation values, and a classical processing unit (CPU) for the variational optimizations. The parametrized quantum circuit is defined by an empirical "ansatz", and thus the ansatz used in the computation determines the accuracy of wave function and energy. Chemists' intuition-oriented ansatzes such as unitary coupled cluster (UCC) ansatz,[11,12] and adaptive derivative-assembled pseudo-Trotter ansatz (ADAPT),[13] qubit coupled cluster,[14] and more heuristic ansatzes called as "hardware-efficient" ones[15] have been well investigated.

So far, a wide variety of theoretical developments have been made in VQE. For example, development of new

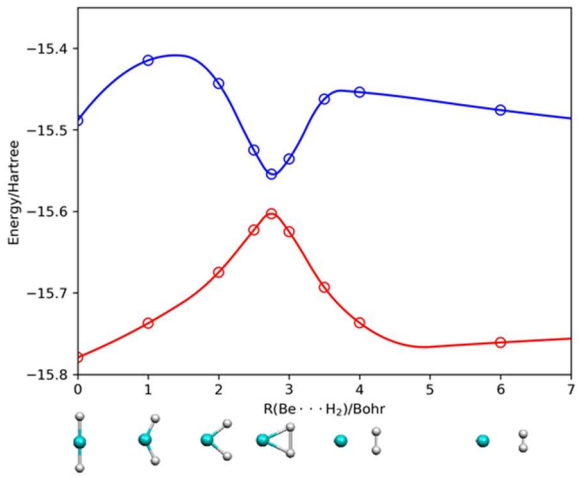

Figure 1. The quasi-reaction pathway being investigated. The horizontal axis represents the distance between Be atom and the centroid of H_2. Red and blue lines specify the potential energy curves of the 1 $^1A_1$ and 2 $^1A_1$ states, respectively. Open circles represent the full-CI energies.

ansatzes,[16–24] qubit reductions by utilizing natural orbitals,[25,26] extension of ansatzes for larger systems,[27–30] introduction of error mitigation techniques,[31–33] spatial and spin symmetry adaptations,[34–37] reduction of the number of qubit measurements,[38–41] applications for electronic excited states,[42–45] and so on. Proof-of-principle demonstrations on quantum devices were also reported.[46–50] Recent reviews in this field can be found elsewhere.[51–55]

From the viewpoint of chemistry, we emphasize that most of problems in chemistry focus on the energy differences between two or larger number of electronic states or geometries, rather than the total energies themselves. To understand chemistry and chemical processes correctly and to make quantum computers useful in the investigations of real-world chemistry problems, calculating various electronic structures and molecular systems with the same accuracy is essential. Most of theoretical studies on the VQE-based energy calculations focuses on the simple potential energy curves by stretching covalent bonds or changing bonding angles, or simple concerted chemical reactions. It is interesting whether VQE is able to correctly describe more complex chemical reactions; for example, reactant and product have different electronic configurations and avoided crossing between the ground and excited states is involved in the reaction pathway. If avoided crossing is present in the reaction process, the wave function around the crossing point cannot be well approximated by a single Slater determinant like Hartree–Fock (HF) and by a single configuration state function (CSF). In such systems both dynamical and static (or non-dynamical) electron correlation effects are prominent, and non-variational single-reference molecular orbital theories such as the second-order Møller–Plesset (MP2) and coupled cluster with singles and doubles (CCSD) becomes less reliable.[56–58]

In this work, we focus on the beryllium atom insertion reaction to H_2 to generate a BeH_2 molecule illustrated in Figure 1 as the representative example of the chemical reactions of which S_0–S_1 avoided crossing is involved. This reaction pathway has been precisely investigated as the model system of multiconfigurational electronic structure treatments.[59–65] As clearly seen in Figure 1, this reaction pathway contains avoided crossing at R(Be···H_2) ~ 2.75 Bohr, and it is a good testing ground for the sophisticated quantum chemical calculations

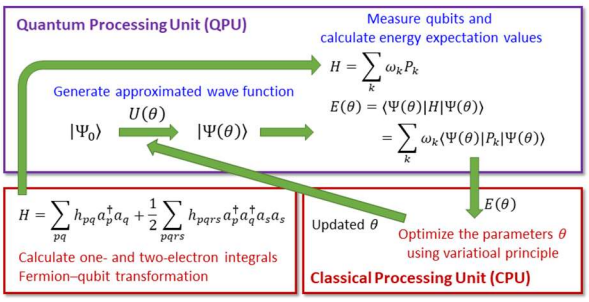

Figure 2. A schematic view of the VQE-based quantum chemical calculations.

using VQE. It should be also noted that this system is illustrative in teaching physical chemistry including molecular orbital theory and valence bond descriptions. We examined numerical simulations of VQE along the quasi-reaction pathway in C_{2v} symmetry by using conventional UCCSD ansatz and a multireference unitary coupled cluster with partially generalized singles and doubles (MR-UCCpGSD) ansatz, focusing on the accuracy of wave functions and energies.

The paper is organized as follows. In the section 2 we briefly review the quantum chemical calculations using VQE, and ansatzes used in VQE. Section 3 summarizes computational conditions for the numerical simulations. Results of the numerical simulations are given in section 4, and summary and future perspectives are given in section 5.

2. Theory

Here we briefly review the theoretical methods for quantum chemical calculations using VQE. The schematic view of the VQE-based quantum chemical calculations is provided in Figure 2. VQE consists of two parts, computations on QPU and those on CPU. QPU repeatedly executes preparation of an approximated wave function using a parametrized quantum circuit and following qubit measurements to calculate an energy expectation value. Information of the energy expectation value is transferred to CPU, and CPU carries out variational optimization of the parameters and convergence check. If the variational calculation did not converge, a set of information of the revised parameters are returned to QPU, and QPU executes evaluation of the energy expectation value using the new parameters.

In order to execute VQE, wave function should be mapped onto qubits. Several approaches for fermion–qubit mapping have been proposed,[4,66–70] and we used a Jordan–Wigner transformation (JWT) in this study.[4,66] In the JWT each qubit possesses an occupation number of particular spin orbital; the qubit is in the $|1\rangle$ state if the spin orbital is occupied, otherwise $|0\rangle$. Electronic Hamiltonian H defined in second quantized formula is given in eq (2), where $a_p^\dagger$ and a_p are creation and annihilation operators, respectively, acting on the p-th spin orbital. h_{pq} and h_{pqrs} are one- and two-electron molecular orbital integrals, respectively, and they are computed on classical computers prior to quantum simulations. By applying the JWT, creation and annihilation operators are transformed to the linear combination of the direct product of Pauli operators, by using eqs (3) and (4).

$$H = \sum_{pq} h_{pq} a_p^\dagger a_q + \frac{1}{2}\sum_{pqrs} h_{pqrs} a_p^\dagger a_q^\dagger a_s a_r \quad (2)$$

$$a_p^\dagger = \frac{1}{2}\left(X_p - iY_p\right)\prod_{t<p} Z_t \quad (3)$$

$$a_p = \frac{1}{2}\left(X_p + iY_p\right)\prod_{t<p} Z_t \quad (4)$$

Here, X_p, Y_p, and Z_p are Pauli operators defined in eqs (5)–

(7), acting on the *p*-th qubit.

$$X = \begin{pmatrix} 0 & 1 \\ 1 & 0 \end{pmatrix} \quad (5)$$

$$Y = \begin{pmatrix} 0 & -i \\ i & 0 \end{pmatrix} \quad (6)$$

$$Z = \begin{pmatrix} 1 & 0 \\ 0 & -1 \end{pmatrix} \quad (7)$$

Under the JWT the electronic Hamiltonian is transformed to a qubit Hamiltonian as in eqs (8) and (9).

$$H = \sum_k w_k P_k \quad (8)$$

$$P_k = \sigma_N \otimes \sigma_{N-1} \otimes \cdots \otimes \sigma_1, \quad \sigma \in \{I, X, Y, Z\} \quad (9)$$

Here, *N* is the number of qubits used for wave function storage. In the JWT *N* equals to the number of spin orbitals included in the active space. The qubit Hamiltonian consists of Pauli operators and its expectation value can be calculated statistically, by repetitively performing wave function preparation and subsequent qubit measurements.

An approximate wave function is generated on QPU by using a parametric quantum circuit defined through an ansatz, and thus selection of appropriate ansatz is the most important process. Ansatzes used in VQE-based quantum chemical calculations can be roughly classified into two categories; chemistry inspired and hardware efficient ones.[55] The most famous chemistry inspired ansatz is the unitary coupled cluster (UCC) ansatz. The UCC wave function is defined as in eqs (10) and (11).[11]

$$|\Psi_{\mathrm{UCC}}\rangle = \exp \tau \, |\Psi_0\rangle = \exp\left(T - T^\dagger\right) |\Psi_0\rangle \quad (10)$$

$$T = \sum_{ia} t_{ia} a_a^\dagger a_i + \sum_{ijab} t_{ijab} a_a^\dagger a_b^\dagger a_j a_i + \cdots \quad (11)$$

In eq (10) $|\Psi_0\rangle$ is the reference wave function and HF wave function $|\Psi_{\mathrm{HF}}\rangle$ is usually used. *T* defined in eq (11) is the operators describing electron excitations from the occupied orbitals to the virtual orbitals in the reference wave function. Throughout this paper we use indices *i*, *j*, and *k* for occupied, *a*, *b*, and *c* for unoccupied, and *p*, *q*, *r*, and *s* for general spin orbitals. We used *u* and *v* for the indices for general molecular orbitals. Compared with the conventional coupled cluster (CC) method, the UCC wave function in eq (10) takes into account electron de-excitations from the unoccupied to occupied orbitals ($T^\dagger$) as well as electron excitations *T*. Calculation of the UCC wave function on a classical computer is difficult, because the Baker–Campbell–Hausdorff (BCH) expansion of the similarly transformed Hamiltonian $e^{-(T-T^\dagger)} H e^{(T-T^\dagger)}$ does not terminate. By contrast, preparation of the UCC wave function on quantum computer is straightforward, because $\exp\left(T - T^\dagger\right)$ is a unitary operator. Since the CCSD(T) (single and double excitation operators are considered, and effects of connected triples are taken into account through many body perturbation theory) method is regarded as the "gold standard" in quantum chemistry, the UCC with singles and doubles (UCCSD) can be a practical tool for reliable quantum chemical calculations on quantum computers. However, it is well known that the approximation of conventional coupled cluster methods like CCSD becomes worse when static electron correlation effect is significant and wave function cannot be well approximated at the HF level. As a result, conventional CCSD cannot describe the potential curve associated to covalent bond dissociation correctly where static correlation is crucial.[57,58] Note that UCCSD on VQE is solved by using variational principle and thus variational collapse never occurs. Nevertheless, it is still unclear whether the UCCSD ansatz can afford to describe electronic structure of strongly correlated systems accurately or not. Following the ab initio molecular orbital theory for classical computers, we expect that multireference extension of the UCCSD ansatz is promising for the description of strongly correlated systems.

So far, ansatzes for VQE with the multireference wave functions have been proposed already.[17,23] Here we examine the most straightforward extension of the UCC ansatz to the multireference regime by using the MR-UCCpGSD ansatz. In the MR-UCCpGSD the reference wave function $|\Psi_0\rangle$ is not a single determinant but a multiconfigurational wave function $|\Psi_{\mathrm{MC}}\rangle$ such as complete active space self-consistent-field (CASSCF) wave functions.[71,72] As the excitation operator *T* we take into account all possible symmetry-adapted single and double excitation operators from each reference Slater determinant included in $|\Psi_{\mathrm{MC}}\rangle$. For example, in this study we used the CASSCF(2e,2o) wave function as the $|\Psi_{\mathrm{MC}}\rangle$, which consists of two Slater determinants: $|2220000000\rangle$ and $|2202000000\rangle$. Here, 2 and 0 specify the occupation number of molecular orbitals. In this case we consider one- and two-electron excitation operators and their complex conjugates from these two determinants. Therefore, in the MR-UCCpGSD calculations up to four-electron excitation operators from the HF configuration is involved. As easily expected, the same excitation operator can be derived from difference reference determinants. In this case we merge the operators and treat them as one excitation operator. Note that the reported multireference ansatz based on unitary coupled cluster generalized singles and doubles (UCCGSD) takes into account occupied → occupied (e.g., $t_{ij} a_j^\dagger a_i$) and unoccupied → unoccupied ($t_{ab} a_b^\dagger a_a$) excitations, in addition to occupied → unoccupied ($t_{ia} a_a^\dagger a_i$) excitations.[17] By contrast, in our formulation of the MR-UCCpGSD, the occupied → occupied and the unoccupied → unoccupied excitations outside of the active space are not included, because these terms have zero contributions to the reference wave function as the connected terms $\tau|\Psi_0\rangle$. They can have nonzero contributions as the disconnected terms such as $(\tau^2/2)|\Psi_0\rangle$ and $(\tau^3/3!)|\Psi_0\rangle$, but we assume that such contributions are small. Thus, the number of variables in MR-UCCpGSD is smaller than that of UCCGSD. In this context we used the term "partially generalized" for the name of ansatz.

Once an energy expectation value is computed on QPU, CPU executes variational optimization of the parameters. In the UCCSD ansatz, the variables are excitation amplitudes t_{ia} and t_{ijab} in eq (11). Variational optimizations are often carried out by using derivative-free algorithms such as Nelder–Mead, Powell, and constrained optimization by linear approximation (COBYLA) methods. These procedures are iterated until achieve convergence.

As naturally expected, variational optimization in VQE cycles converges faster if the initial estimates of the parameters are closer to the optimal values. In the UCCSD ansatz, an approach to use the MP2 amplitudes given in eq (12) as the initial amplitudes was proposed.[73]

$$t_{ijab} = \frac{h_{ijba} - h_{ijab}}{\varepsilon_i + \varepsilon_j - \varepsilon_a - \varepsilon_b} \quad (12)$$

In the MP2 framework one electron excitation amplitudes t_{ia} are zero due to Brillouin's theorem.[5] However, if we consider the second order wave function in the perturbation theory, we can derive the following equation, which can be used as the initial estimate of t_{ia} amplitudes.[74] Note that in the presence of non-dynamical electron correlation, the reorganization from the HF description should be substantial through sizable contributions from single excitations.[75,76] We expect that

nonzero t_{ia} initial amplitudes can accelerate the convergence of VQE, especially when static electron correlation is prominent.

$$t_{ia}(\text{unscaled}) = \frac{\sum_{jbc} 2t_{ijcb}h_{jabc} - \sum_{jkb} 2t_{jkba}h_{jikb}}{\varepsilon_i - \varepsilon_a} \quad (13)$$

Using a partial renormalization with size-consistency,[77] the following scaled amplitudes are also tested.

$$t_{ia}(\text{scaled}) = \frac{t_{ia}(\text{unscaled})}{1+\sum_b\{t_{ib}(\text{unscaled})\}^2} \quad (14)$$

Importantly, only the spatial symmetry-adapted excitation operators have nonzero amplitudes by adopting the initial amplitude estimation methods described here. Excitation operators giving zero initial amplitudes have no contribution to the ground state wave function when they appear in the connected terms. Thus, application of perturbation theory-based initial amplitude estimation is useful not only to find good initial estimates of variables but also to automatically select excitation operators those give nonzero contribution to the ground state wave function. For the MR-UCCpGSD calculations, we extended the initial amplitude estimation technique described above to the multireference regime as follows. Assume that the reference wave function is described by a linear combination of Slater determinants as in eq (15). The initial amplitudes for MR-UCCpGSD can be computed by a linear combination of the product of the CI expansion coefficient c_l and the MP2 amplitudes computed by using each Slater determinant as in eq (16), for two electron excitation amplitudes, for example.

$$|\Psi_{\text{MC}}\rangle = \sum_l c_l |\Phi_l\rangle \quad (15)$$

$$t_{ijab}(\text{MC}) = \sum_l c_l t_{ijab}(\Phi_l) \quad (16)$$

Calculations of the amplitudes $t_{ijab}(\Phi_l)$ using eqs (12)–(14) requires orbital energies. We used the CASSCF canonical orbital energies for the $1\ ^1A_1$ ground state for the initial amplitude estimations.

Because molecules exhibit different molecular properties at different spin multiplicities, spin symmetry-adapted treatment is very important in quantum chemical calculations. Spin symmetry adaptation can be accomplished by considering the spin symmetry-adapted excitation operators for the singlet defined in eq (15).

$$T_{uv} = \frac{t_{uv}}{\sqrt{2}}\left(a^\dagger_{v\alpha}a_{u\alpha} + a^\dagger_{v\beta}a_{u\beta}\right) \quad (15)$$

In the UCCSD and MR-GCCpGSD ansatzes the spin symmetry adaptation can be done by using the same excitation amplitudes for the spin $\alpha \rightarrow \alpha$ and $\beta \rightarrow \beta$ excitations, as in eq (16).

$$t_{u\alpha\rightarrow v\alpha} = t_{u\beta\rightarrow v\beta} \quad (16)$$

3. Computational conditions

In this study we calculated ten geometries along the sampling path for the C_{2v} potential energy surface, by following the previous study by Purvis and coworkers.[60] Cartesian coordinate of H atoms are listed in Table 1. Here, Be atom is located at the origin of coordinate (0.0, 0.0, 0.0). We used the same basis set as the study by Purvis and coworkers,[60] which is comprised of (10s 3p)/[3s 1p] for Be and (4s)/[2s] for H. The exponents and contraction coefficients for the basis set is given in Supporting Information (SI). The wave function is mapped onto 20 qubits by using this basis set.

For the numerical simulations of the VQE-based UCCSD and MR-UCCpGSD calculations we developed a python program by utilizing OpenFermion[78] and Cirq[79] libraries. We used a quantum state vector simulator to calculate the energy expectation value, which corresponds to infinite number of repetitive measurements. Needless to say, in the real quantum devices only finite number of measurements are available, but we are interested in the accuracy and the validity of the ansatz, and hence quantum state vector simulator is more suitable for this purpose. The quantum circuits for the UCCSD and MR-UCCpGSD ansatzes are constructed by adopting the first order Trotter decomposition with the Trotter slice number $n = 1$. The HF calculations and computations of one- and two-electron atomic orbital integrals were performed by using GAMESS-US program package.[80] One- and two-electron molecular orbital integrals were prepared by using our own AO→MO integral transformation program.

Table 1. Cartesian coordinates of H atoms for the points being investigated, in unit of Bohr.

Point	X	Y	Z
A	0.0	±2.540	0.00
B	0.0	±2.080	1.00
C	0.0	±1.620	2.00
D	0.0	±1.390	2.50
E	0.0	±1.275	2.75
F	0.0	±1.160	3.00
G	0.0	±0.930	3.50
H	0.0	±0.700	4.00
I	0.0	±0.700	6.00
J	0.0	±0.700	20.00

Selection of the appropriate optimization algorithm for variational optimization of parameters is another important process to rapidly achieve the variational minima. In this work we carried out preliminary VQE-UCCSD/STO-3G simulations of a LiH molecule with R(Li–H) = 1.0, 2.0, 3.0, and 4.0 Å using Nelder–Mead, Powell, and COBYLA algorithms for the parameter optimizations. Our simulations revealed that COBYLA exhibits the fastest convergence behavior among three algorithms. Also, Nelder–Mead sometimes trapped to a local minimum and gives rise to larger deviation in energy from the full-CI value. Details of the numerical simulations of LiH are given in SI. We adopted the COBYLA algorithm for the VQE-UCCSD and MR-UCCpGSD simulations.

4. Results and Discussion

The deviations of the energy expectation values calculated at the RHF, CASSCF(2e, 2o), UCCSD, and MR-UCCpGSD methods from the full-CI one is illustrated in Figure 3a, and the square overlap between the approximated and the full-CI wave functions are plotted in Figure 3b. The values of the HF, CASSCF, UCCSD, MR-UCCpGSD, and full-CI energies are summarized in Table S1 in SI. We also confirmed that the HF and full-CI energies computed in this work coincides to the values reported by Purvis and coworkers.[60] Note that we set the number of maximum iterations in the variational optimization to be 10000, but the UCCSD simulations did not converge after 10000 iterations for points D, E, and F. As clearly seen in Figure 3, the UCCSD method gives the energy close to the full-CI one for all points except for point E. The point E corresponds to the transition structure of the reaction pathway under study, and it is closest to the point where the avoided crossing occurs. The square overlap between the HF and the full-CI wave functions are calculated to be 0.524, and thus the HF wave function is not a good approximation for the electronic ground state. We also checked stability of the HF wave function[81] at points D, E, and F, observing the triplet instabilities at these points, and singlet instability at point E (see SI for details). The deviation of the UCCSD energy from the full-CI one is 0.263, 7.360, and 0.056 kcal mol^{-1} for points A, E, and J, respectively. As a result, the UCCSD method overestimates the reaction energy barrier about 7.0 kcal mol^{-1} from the full-CI.

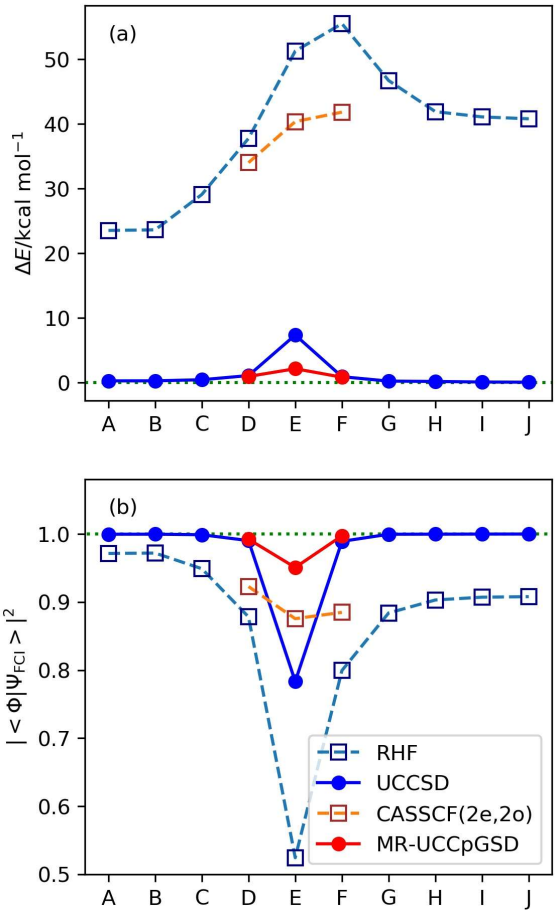

Figure 3. Results of the numerical quantum circuit simulations. (a) The deviations of the computed energy from the full-CI value, (b) The square overlap with the full-CI wave function.

Convergence behaviors of the VQE-UCCSD simulations are plotted in Figure 4. The VQE-UCCSD converges very slowly at point E, and it is far from the full-CI wave function even after 10000 iterations. To estimate the number of iterations required to achieve convergence, we attempted to fit the energy difference plot in the range between 1000 to 10000 iterations with an exponential function, obtaining $\Delta E = 123.68x^{-0.303}$ with $R^2 = 0.9827$ (see SI for details). Needless to say, there is no theoretical background for the energy change in the optimizations to be in the form of an exponential function. However, if we assume that the VQE optimization proceeds along the exponential function, we need about 8000000 iterations to achieve 1.0 kcal mol^{-1} of deviation from the full-CI value. It should also be noted that the square overlap between the UCCSD and the full-CI wave functions is at most 0.783 even after 10000 iterations at point E. These results clearly exemplify the fact that convergence of the UCCSD ansatz is very slow if the square overlap between the reference and full-CI wave functions is small. Using good reference function having sufficiently large overlap with the full-CI wave function might be more important than we expected.

It is unclear whether the large deviation of the UCCSD energy from the full-CI value at point E is due to extremely slow convergence behavior or due to the limitation of the representability of the UCCSD ansatz. Because following the convergence by increasing the number of iterations is impractical, we examined the UCCSD simulations at point E by using the STO-3G basis set. The number of variables is reduced from 151 to 44 by employing the STO-3G basis set. VQE optimization converges faster for smaller number of variables, and therefore simulations using the STO-3G basis helps us to investigate two possible mechanisms described above in more detail. The UCCSD/STO-3G simulation converged after 3329 iterations, giving $\Delta E_{\text{UCCSD–full-CI}} = 2.866$ kcal mol^{-1} and $|\langle\Psi_{\text{UCC}}|\Psi_{\text{full-CI}}\rangle|^2 = 0.963$. From this result the UCCSD seems to give accurate energy if the sufficient number of iterations are possible. By adopting the MR-UCCpGSD ansatz described below to the calculation of point E with the STO-3G basis set, we obtained $\Delta E_{\text{MR-UCCpGSD–full-CI}} = 1.039$ kcal mol^{-1} and $|\langle\Psi_{\text{MR-UCCpGSD}}|\Psi_{\text{full-CI}}\rangle|^2 = 0.992$. This result claims that representability of the ansatz is also responsible for the rather poor result of the UCCSD calculation and importance of the multiconfigurational approach for strongly correlated systems.

We also checked the dependence of the UCCSD energies and convergence behaviors against initial estimate of the one-electron excitation amplitudes t_{ia}, but no significant initial guess dependences have been observed (see Figure 5 for point E and Figure S6 in SI for points A, D, F, and I).

Because the single-reference UCCSD seems to be no more an appropriate choice for the calculations of strongly correlated systems, adopting the multireference flamework is a natural choice for the alternative. One of the author proposed a theoretical method to generate the multiconfigurational wave functions on quantum computers by utilizing the diradical characters y computed from the broken-symmetry spin-unrestricted Hartree–Fock (BS-UHF) wave functions.[82] First, we computed the energy expectation values and square overlaps with the full-CI wave functions of the two-configurational wave functions constructed by following the approach described in the reference.[82] The results are summarized in Table 2. The BS-UHF computations converged to the closed-shell RHF wave function at points A, B, I, and J.

Table 2. Diradical character y, energy differences, and the square overlaps computed by using the two configurational wave function $|\Psi_{2c}\rangle$

Point	y	$\Delta E_{2c-\text{full-CI}}$ /kcal mol^{-1}	$\lvert\langle\Psi_{2c}\rvert\Psi_{\text{full-CI}}\rangle\rvert^2$
C	0.0008	28.536	0.952
D	0.2991	35.591	0.933
E	0.7851	43.553	0.905
F	0.6125	48.498	0.886
G	0.0373	42.417	0.903
H	0.0007	40.998	0.906

Noticeably, the two configurational wave function constructed by using the diradical character y has larger square overlap with the full-CI wave function compared with the UCCSD wave function after 10000 iterations at point E, although the energy difference between the two configurational wave function and the full-CI is notably large, due to lack of dynamical electron correlation effect. One of the anticipated application of VQE is the preparation of approximate wave functions for the input of QPE-based full-CI. QPE utilizes a projective measurement to obtain t he eigenenergy of the second-quantized Hamiltonian, namely the full-CI energy, and therefore using the wave function having large overlap with the full-CI is very important.[4] In this context, conventional UCCSD is less appropriate than the two-configurational wave functions constructed by using the diradical characters for the initial wave functions of QPE.[82] We attempted to carry out VQE simulations with the MR-UCCpGSD ansatz for the points D, E, and F, those have large diradical characters. However, using the two configurational wave functions directly as the reference wave

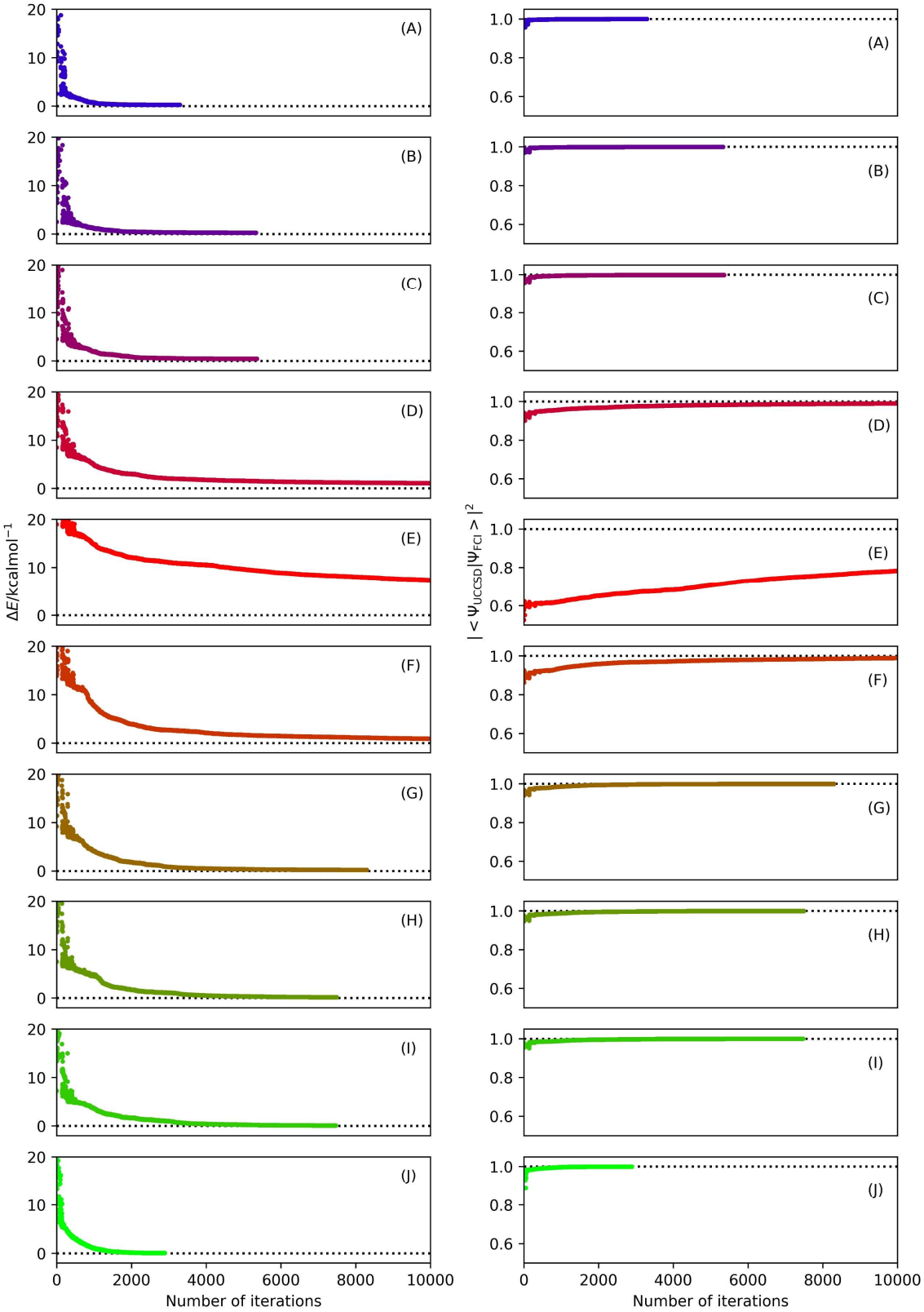

Figure 4. Convergence behaviors of the VQE-UCCSD simulations. The difference between UCCSD and full-CI energies (left) and the square overlap between UCCSD and full-CI wave functions (right).

functions in the MR-UCCpGSD simulations is not plausible, because the two-configurational wave functions constructed by utilizing the diradical character y are not spatial symmetry adapted, and therefore the number of excitation operators with nonzero contributions to the electronic ground state will increase. Instead, we performed the CASSCF(2e,2o) calculations and use the CASSCF wave function as the reference in the MR-UCCpGSD calculations. The MR-UCCpGSD results are also plotted in Figure 3, and the convergence behaviors of the UCCSD and MR-UCCpGSD calculations at point E are summarized in Figure 5. The energy expectation value at point E drastically improved by adopting the multireference approach. After 10000 iterations, the deviation from the full-CI energy is calculated to be 2.143 kcal mol^{-1} and $\langle \Psi_{\text{MR-UCCpGSD}} | \Psi_{\text{full-CI}} \rangle|^2 =$

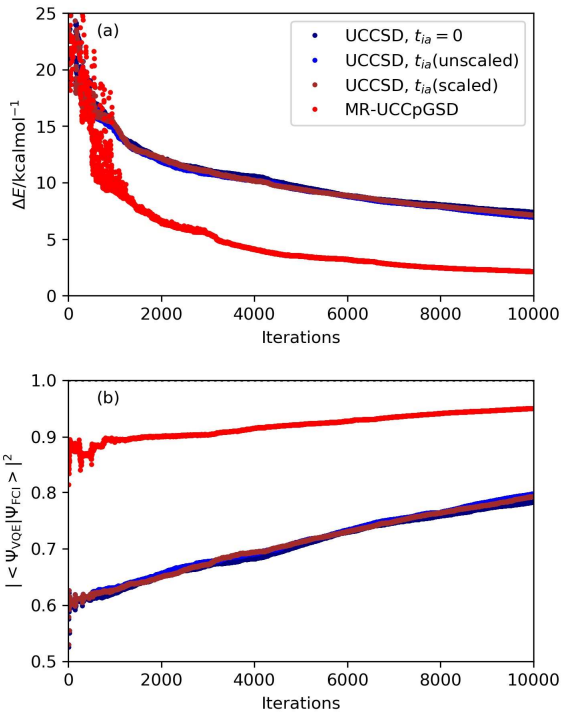

Figure 5. Convergence behaviors of the VQE-UCCSD and MR-UCCpGSD simulations. (a) The energy difference from the full-CI and (b) the square overlap with the full-CI wave function.

0.950. By fitting the plot of energy difference with an exponential function, we obtained $\Delta E = 1289.2x^{-0.693}$ with $R^2 = 0.9932$. From this, we expect that about 30000 iterations are needed to achieve the energy deviation from the full-CI within 1 kcal mol^{-1}. This value should be compared with ca. 8000000 iterations in conventional single-reference UCCSD. However, 30000 iterations are still too many for practical use. It should be also noted that our simulations are based on the quantum state vector simulator that corresponds to infinite number of repetitive measurements for the calculations of energy expectation values. Implementation of methods that can accelerate convergence behavior and reduce the number of iterations, or application of more sophisticated optimization algorithms such as an approach to calculate analytical gradients by adopting parameter shift rule[83] or DIIS-based algorithm[84] is essential for the practical use of VQE for quantum chemical calculations. Another possible approach to improve the convergence behavior is adopting the sequential optimization approaches. Nevertheless, it should be emphasized that the MR-UCCpGSD ansatz shows faster convergence behavior compared with UCCSD at strongly correlated systems and it can give more reliable wave function. Multiconfigurational treatment is quite powerful to study the strongly correlated systems on quantum computers.

5. Summary

In this work, we carried out numerical simulations of VQE for the quasi-reaction pathway in C_{2v} symmetry of the Be atom insertion to H_2 molecule, focusing on the accuracy of the wave function at the geometry nearby an avoided crossing point and accuracy of the reaction energetics. Conventional single-reference UCCSD shows extremely slow convergence behavior at the quasi-transition structure, and the UCCSD energy obtained from VQE simulations after 10000 iterations is 7.360 kcal mol^{-1} overestimated from the full-CI value. As a result, conventional UCCSD overestimates the potential energy barrier of the Be insertion reaction about 7 kcal mol^{-1}. The square overlap between the UCCSD and full-CI wave functions is at most 0.783 at point E, which is smaller than the square overlaps with the full-CI wave function calculated by using the two-configurational wave function constructed by using the diradical character *y*. The UCCSD ansatz is not a proper choice for the study of strongly correlated systems, even for the purpose of preparing initial wave function for the QPE-based full-CI.

By contrast, the MR-UCCpGSD gives the energy much closer to the full-CI one at the geometry nearby the avoided crossing, exemplifying that the multireference treatment is more feasible for the accurate descriptions of the electronic structures of strongly correlated systems. At the MR-UCCpGSD level of theory, the reaction energy barrier is still overestimated, but significant improvement of the transition energy is observed by applying the multireference approach.

There are many molecular systems those both dynamical and static electron correlation effects play significant roles, such as electronic ground state of ozone,[85] the out-of-plane transition state of the cis–trans isomerization reaction of diazene,[86] zigzag edges of graphene nanoribbons,[87] and so on. Molecules having such complicated electronic structures are the systems of which sophisticated quantum chemical calculations are truly desirable, and thus importance of multireference treatments cannot be overemphasized. Applications of the MR-UCCpGSD ansatz for other strongly correlated systems are ongoing and will be discussed in the forthcoming paper.

Acknowledgement

This work was supported by JSPS KAKENHI Scientific Research C (Grant No. 18K03465 and 21K03407). K.S. acknowledges the support from JST PREST project "Quantum Software" (JPMJPR1914).

References

1. P. W. Shor, Algorithms for quantum computation: discrete logarithms and factoring, in *Proc. 35th Ann. Symp. on the Foundations of Computer Science*, S. Goldwasser, Ed., IEEE Computer Society Press, Los Alamitos, California, 1994, pp. 124–134.
2. K. K. H. Cheung, M. Mosca, Decomposing finite Abelian groups, *Quantum Info. Comp.* **2001**, *1(3)*, 26–32.
3. M. A. Nielsen, I. L. Chuang, *Quantum Computation and Quantum Information, 10th Anniversary Edition*, Cambridge University Press, New York, 2010.
4. A. Aspuru-Guzik, A. D. Dutoi, P. J. Love, M. Head-Gordon, Simulated quantum computation of molecular energies, *Science*, **2005**, *309*, 1704–1707.
5. A. Szabo, N. S. Ostlund, *Modern Quantum Chemistry: Introduction to Advanced Electronic Structure Theory.* Dover Publications, Inc., New York, 1996.
6. B. P. Lanyon, J. D. Whitfield, G. G. Gillett, M. E. Goggin, M. P. Almeida, I. Kassal, J. D. Biamonte, M. Mohseni, B. J. Powell, M. Barbieri, A. Aspuru-Guzik, A. G. White, Towards quantum chemistry on a quantum computer, *Nat. Chem.* **2010**, *2*, 106–111.
7. J. Du, N. Xu, X. Peng, P. Wang, S. Wu, D. Lu, NMR implementation of a molecular hydrogen quantum simulation with adiabatic state preparation, *Phys. Rev. Lett.* **2010**, *104*, 030502.
8. M.-H. Yung, J. Casanova, A. Mezzacapo, J. McClean, L. Lamata, A. Aspuru-Guzik, E. Solano, From transistor to trapped-ion computers for quantum chemistry, *Sci. Rep.* **2014**, *4*, 3589.
9. A. Peruzzo, J. McClean, P. Shadbolt, M.-H. Yung, X.-Q.

Zhou, P. J. Love, A. Aspuru-Guzik, J. L. O'Brien, A variational eigenvalue solver on a photonic quantum processor, *Nat. Comm.* **2014**, *5*, 4213.
10. J. Preskill, Quantum computing in the NISQ era and beyond, *Quantum*, **2018**, *2*, 79.
11. A. G. Taube, R. J. Bartlett, New perspectives on unitary coupled-cluster theory, *Int. J. Quantum Chem.* **2006**, *106*, 3393–3401.
12. F. A. Evangelista, G. K.-L. Chan, G. E. Scuseria, Exact parametrization of fermionic wave functions via unitary coupled cluster theory, *J. Chem. Phys.* **2019**, *151*, 244112.
13. H. R. Grimsley, S. E. Economou, E. Barnes, N. J. Mayhall, An adaptive variational algorithm for exact molecular simulations on a quantum computer, *Nat. Comm.* **2019**, *10*, 3007.
14. I. G. Ryabinkin, T.-C. Yen, S. N. Genin, A. F. Izmaylov, Qubit coupled cluster method: A systematic approach to quantum chemistry on a quantum computer, *J. Chem. Theory Comput.* **2018**, *14*, 6317–6326.
15. A. Kandala, A. Mezzacapo, K. Temme, M. Takita, M. Brink, J. M. Chow, J. M. Gambetta, Hardware-efficient variational quantum eigensolver for small molecules and quantum magnets, *Nature*, **2017**, *549*, 242–246.
16. P. K. Barkoutsos, J. F. Gonthier, I. Sokolov, N. Moll, G. Salis, A. Fuhrer, M. Ganzhorn, D. J. Egger, M. Troyer, A. Mezzacapo, S. Filipp, I. Tavernelli, Quantum algorithms for electronic structure calculations: Particle–hole Hamiltonian and optimized wave-function expansions. *Phys. Rev. A* **2018**, *98*, 022322.
17. J. Lee, W. J. Huggins, M. Head-Gordon, K. B. Whaley, Generalized unitary coupled cluster wave functions for quantum computation, *J. Chem. Theory Comput.* **2019**, *15*, 311–324.
18. P.-L. Dallaire-Demers, J. Romero, L. Veis, S. Sim, A. Aspuru-Guzik, Low-depth circuit ansatz for preparing correlated fermionic states on a quantum computer, *Quantum Sci. Technol.* **2019**, *4*, 045005.
19. W. Mizukami, K. Mitarai, Y. O. Nakagawa, T. Yamamoto, T. Yan, Y. Ohnishi, Orbital optimized unitary coupled cluster theory for quantum computer, *Phys. Rev. Research* **2020**, *2*, 033421.
20. I. O. Sokolov, P. K. Barkoutsos, P. J. Ollitrault, D. Greenberg, J. Rice, M. Pistoia, I. Tavernelli, Quantum orbital-optimized unitary coupled cluster method in the strongly correlated regime: Can quantum algorithms outperform their classical equivalents? *J. Chem. Phys.* **2020**, *152*, 124107.
21. Y. Matsuzawa, Y. Kurashige, Jastrow-type decomposition in quantum chemistry for low-depth quantum circuits, *J. Chem. Theory Comput.* **2020**, *16*, 944–952.
22. I. G. Ryabinkin, R. A. Lang, S. N. Genin, A. F. Izmaylov, Iterative qubit coupled cluster approach with efficient screening of generators, *J. Chem. Theory Comput.* **2020**, *16*, 1055–1063.
23. N. H. Stair, R. Huang, F. A. Evangelista, A multireference quantum Krylov algorithm for strongly correlated electrons, *J. Chem. Theory Comput.* **2020**, *16*, 2236–2245.
24. M. Metcalf, N. P. Bauman, K. Kowalski, W. A. de Jong, Resource efficient chemistry on quantum computers with the variational quantum eigensolver and the double unitary coupled-cluster approach, *J. Chem. Theory Comput.* **2020**, *16*, 6165–6175.
25. Y. Mochizuki, K. Okuwaki, T. Kato, Y. Minato, Reduction of orbital space for molecular orbital calculations with quantum computation simulator for educations, chemRxiv, Preprint, https://doi.org/10.26434/chemrxiv.9863810.v1
26. P. Verma, L. Huntington, M. Coons, Y. Kawashima, T. Yamazaki, A. Zaribafiyan, Scaling up electronic structure calculations on quantum computers: The frozen natural orbital based method of increments, arXiv:2002.07901.
27. N. C. Rubin, A hybrid classical/quantum approach for large-scale studies of quantum systems with density matrix embedding theory, arXiv:1610.06910.
28. T. Yamazaki, S. Matsuura, A. Narimani, A. Saidmuradov, A. Zaribafiyan, Towards the practical application of near-term quantum computers in quantum chemistry simulations: A problem decomposition approach, arXiv:1806.01305.
29. T. Takeshita, N. C. Rubin, Z. Jiang, E. Lee, R. Babbush, J. R. McClean, Increasing the representation accuracy of quantum simulations of chemistry without extra quantum resources, *Phys. Rev. X* **2020**, *10*, 011004.
30. K. Fujii, K. Mitarai, W. Mizukami, Y. O. Nakagawa, Deep variational quantum eigensolver: a divide-and-conquer method for solving a larger problem with smaller size quantum computers. arXiv:2007.10917.
31. J. R. McClean, M. E. Kimchi-Schwartz, J. Carter, W. A. de Jong, Hybrid quantum–classical hierarchy for mitigation of decoherence and determination of excited states, *Phys. Rev. A* **2017**, *95*, 042308.
32. S. Endo, S. C. Benjamin, Y. Li, Practical quantum error mitigation for near-future applications, *Phys. Rev. X* **2018**, *8*, 031027.
33. R. Sagastizabal, X. Bonet-Monroig, M. Singh, M. A. Rol, C. C. Bultink, X. Fu, C. H. Price, V. P. Ostroukh, N. Muthusubramanian, A. Bruno, M. Beekman, N. Haider, T. E. O'Brien, L. DiCarlo, Experimental error mitigation via symmetry verification in a variational quantum eigensolver, *Phys. Rev. A* **2019**, *100*, 010302.
34. I. G. Ryabinkin, S. N. Genin, Symmetry adaptation in quantum chemistry calculations on a quantum computer, arXiv:1812.09812.
35. T. Tsuchimochi, Y. Mori, S. L. Ten-no, Spin projection for quantum computation: A low-depth approach to strong correlation, *Phys. Rev. Research* **2020**, *2*, 043142.
36. B. T. Gard, L. Zhu, G. S. Barron, N. J. Mayhall, S. E. Economou, E. Barnes, Efficient symmetry-preserving state preparation circuits for the variational quantum eigensolver algorithm, *npj Quantum Info.* **2020**, *6*, 10.
37. K. Setia, R. Chen, J. E. Rice, A. Mezzacapo, M. Pistoia, J. D. Whitfield, Reducing qubit requirements for quantum simulations using molecular point group symmetries, *J. Chem. Theory Comput.* **2020**, *16*, 6091–6097.
38. A. F. Izmaylov, T.-C. Yen, I. G. Ryabinkin, Revisiting the measurement process in the variational quantum eigensolver: is it possible to reduce the number of separately measured operators? *Chem. Sci.* **2019**, *10*, 3746–3755.
39. P. Gokhale, O. Angiuli, Y. Ding, K. Gui, T. Tomesh, M. Suchara, M. Martonosi, F. T. Chong, $O(N^3)$ measurement cost for variational quantum eigensolver on molecular Hamiltonians, in *IEEE Transactions on Quantum Engineering*, **2020**, *1*, 1–24.
40. A. Zhao, A. Tranter, W. M. Kirby, S. F. Ung, A. Miyake, P. J. Love, Measurement reduction in variational quantum algorithms, *Phys. Rev. A* **2020**, *101*, 062322.
41. V. Verteletskyi, T.-C. Yen, A. F. Izmaylov, Measurement optimization in the variational quantum eigensolver using a minimum clique cover, *J. Chem. Phys.* **2020**, *152*, 124114.
42. K. M. Nakanishi, K. Mitarai, K. Fujii, Subspace-search variational quantum eigensolver for excited states, *Phys.*

Rev. Research **2019**, *1*, 033062.
43. O. Higgott, D. Wang, S. Brierley, Variational quantum computation of excited states, *Quantum* **2019**, *3*, 156.
44. R. M. Parrish, E. G. Hohenstein, P. L. McMahon, T. J. Martínez, Quantum computation of electronic transitions using a variational quantum eigensolver, *Phys. Rev. Lett.* **2019**, *122*, 230401.
45. P. J. Ollitrault, A. Kandala, C.-F. Chen, P. K. Barkoutsos, A. Mezzacapo, M. Pistoia, S. Sheldon, S. Woerner, J. Gambetta, I. Tavernelli, Quantum equation of motion for computing molecular excitation energies on a noisy quantum processor, *Phys. Rev. Research* **2020**, *2*, 043140.
46. P. J. J. O'Malley, R. Babbush, I. D. Kivlichan, J. Romero, J. R. McClean, R. Barends, J. Kelly, P. Roushan, A. Tranter, N. Ding, B. Campbell, Y. Chen, Z. Chen, B. Ciaro, A. Dunsworth, A. G. Fowler, E. Jeffrey, E. Lucero, A. Megrant, J. Y. Mutus, M. Neeley, C. Neill, C. Quintana, D. Sank, A. Vainsencher, J. Wenner, T. C. White, P. V. Coveney, P. J. Love, H. Neven, A. Aspuru-Guzik, J. M. Martinis, Scalable quantum simulation of molecular energies, *Phys. Rev. X* **2016**, *6*, 031007.
47. C. Hempel, C. Maier, J. Romero, J. McClean, T. Monz, H. Shen, P. Jurcevic, B. P. Lanyon, P. Love, R. Babbush, A. Aspuru-Guzik, R. Blatt, C. F. Roos, Quantum chemistry calculations on a trapped-ion quantum simulator, *Phys. Rev. X* **2018**, *8*, 031022.
48. F. Arute, et al. Hartree–Fock on a superconducting qubit quantum computer, *Science* **2020**, *369*, 1084–1089.
49. J. E. Rice, T. P. Gujarati, M. Motta, T. Y. Takeshita, E. Lee, J. A. Latone, J. M. Garcia, Quantum computation of dominant products in lithium-sulfur batteries, *J. Chem. Phys.* **2021**, *154*, 134115.
50. Q. Gao, H. Nakamura, T. P. Gujarati, G. O. Jones, J. E. Rice, S. P. Wood, M. Pistoia, J. M. Garcia, N. Yamamoto, Computational investigations of the lithium superoxide dimer rearrangement on noisy quantum devices, *J. Phys. Chem. A* **2021**, *125*, 1827–1836.
51. Y. Cao, J. Romero, J. P. Olson, M. Degroote, P. D. Johnson, M. Kieferová, I. D. Kivlichan, T. Menke, B. Peropadre, N. P. D. Sawaya, S. Sim, L. Veis, A. Aspuru-Guzik, Quantum chemistry in the age of quantum computing, *Chem. Rev.* **2019**, *119*, 10856–10915.
52. S. McArdle, S. Endo, A. Aspuru-Guzik, S. C. Benjamin, X. Yuan, Quantum computational chemistry, *Rev. Mod. Phys.* **2020**, *92*, 015003.
53. B. Bauer, S. Bravyi, M. Motta, G. K.-L. Chan, Quantum algorithms for quantum chemistry and quantum materials science, *Chem. Rev.* **2020**, *120*, 12685–12717.
54. Y. Li, J. Hu, X.-M. Zhang, Z. Song, M.-H. Yung, Variational quantum simulation for quantum chemistry, *Adv. Theory Simul.* **2019**, *2*, 1800182.
55. D. A. Fedorov, B. Peng, N. Govind, Y. Alexeev, VQE method: A short survey and recent developments, arXiv:2103.08505.
56. H. B. Schlegel, Potential energy curves using unrestricted Møller–Plesset perturbation theory with spin annihilation, *J. Chem. Phys.* **1986**, *84*, 4530–4534.
57. W. D. Laidig, P. Saxe, R. J. Bartlett, The description of N_2 and F_2 potential energy surfaces using multireference coupled cluster theory, *J. Chem. Phys.* **1987**, *86*, 887.
58. I. W. Bulik, T. M. Henderson, G. E. Scuseria, Can single-reference coupled cluster theory describe static correlation? *J. Chem. Theory Comput.* **2015**, *11*, 3171–3179.
59. G. D. Purvis III, R. J. Bartlett, A full coupled-cluster singles and doubles model: The inclusion of disconnected triples, *J. Chem. Phys.* **1982**, *76*, 1910–1918.
60. G. D. Purvis III, R. Shepard, F. B. Brown, R. J. Bartlett, C_{2v} insertion pathway for BeH_2: A test problem for the coupled-cluster single and double excitation model, *Int. J. Quantum Chem.* **1983**, *23*, 835–845.
61. D. O'Neal, H. Taylor, J. Simons, Potential surface walking and reaction paths for C_{2v} Be + H_2 ← BeH_2 → Be + 2H ($^1A_1$), *J. Phys. Chem.* **1984**, *88*, 1510–1513.
62. H. Nakano, Quasidegenerate perturbation theory with multiconfigurational self-consistent field reference functions, *J. Chem. Phys.* **1993**, *99*, 7983.
63. U. S. Mahapatra, B. Datta, D. Mukherjee, A size-consistent state-specific multireference coupled cluster theory: Formal developments and molecular applications, *J. Chem. Phys.* **1999**, *110*, 6171.
64. U. S. Mahapatra, B. Datta, D. Mukherjee, Molecular applications of a size-consistent state-specific multireference perturbation theory with relaxed model-space coefficients, *J. Phys. Chem. A* **1999**, *103*, 1822–1830.
65. D. Pahari, S. Chattopadhyay, S. Das, D. Mukherjee, U. S. Mahapatra, Size-consistent state-specific multi-reference methods: a survey of some recent developments, in *Theory and Applications of Computational Chemistry: The First Forty Years*, C. E. Dykstra, G. Frenking, K. S. Kim, G. E. Scuseria, Eds, Elsevier, Amsterdam, 2005, chapter 22, pp. 581–633.
66. G. Ortiz, J. E. Gubernatis, E. Knill, R. Laflamme, Quantum algorithms for fermionic simulations, *Phys. Rev. A* **2001**, *64*, 022319.
67. J. T. Seeley, M. J. Richard, P. J. Love, The Bravyi–Kitaev transformation for quantum computation of electronic structure, *J. Chem. Phys.* **2012**, *137*, 224109.
68. S. Bravyi, J. M. Gambetta, A. Mezzacapo, K. Temme, Tapering off qubits to simulate fermionic Hamiltonians, arXiv:1701.08213.
69. K. Setia, J. D. Whitfield, Bravyi–Kitaev superfast simulation of electronic structure on a quantum computer, *J. Chem. Phys.* **2018**, *148*, 164104.
70. M. Steudtner, S. Wehner, Quantum codes for quantum simulation of fermions on a square lattice of qubits, *Phys. Rev. A* **2019**, *99*, 022308.
71. B. O. Roos, P. Linse, P. E. M. Siegbahn, M. R. A. Blomberg, A simple method for the evaluation of the second-order-perturbation energy from external double-excitations with a CASSCF reference wavefunction. *Chem. Phys.* **1982**, *66*, 197–207.
72. K. Andersson, P.-Å. Malmqvist, B. O. Roos, Second-order perturbation theory with a complete active space self-consistent field reference function. *J. Chem. Phys.* **1992**, *96*, 1218–1226.
73. J. Romero, R. Babbush, J. R. McClean, C. Hempel, P. J. Love, A. Aspuru-Guzik, Strategies for quantum computing molecular energies using the unitary coupled cluster ansatz, *Quantum Sci. Technol.* **2018**, *4*, 014008.
74. Y. Mochizuki, K. Tanaka, Modification for spin-adapted version of configuration interaction singles with perturbative doubles. *Chem. Phys. Lett.* **2007**, *443*, 389–397.
75. T. J. Lee, P. R. Taylor, A diagnostic for determining the quality of single-reference electron correlation methods. *Int. J. Quantum Chem.* **1989**, *36*, 199–207.
76. T. J. Lee, A. P. Rendell, P. R. Taylor, Comparison of the quadratic configuration interaction and coupled-cluster approaches to electron correlation including the effect of triple excitations. *J. Phys. Chem.* **1990**, *94*, 5463–5468.
77. Y. Mochizuki, A size-extensive modification of super-CI

for orbital relaxation. *Chem. Phys. Lett.* **2005**, *410*, 165–171.

78. J. R. McClean, N. C. Rubin, K. J. Sung, I. D. Kivlichan, X. Bonet-Monroig, Y. Cao, C. Dai, E. Schuyler Fried, C. Gidney, B. Gimby, P. Gokhale, T. Häner, T. Hadikar, V. Havlíček, O. Higgott, C. Huang, J. Izaac, Z. Jiang, X. Liu, S. McArdle, M. Neeley, T. O'Brien, B. O'Gorman, I. Ozfidan, M. D. Radin, J. Romero, N. P. D. Sawaya, B. Senjean, K. Setia, S. Sim, D. S. Steiger, M. Steudtner, Q. Sun, W. Sun, D. Wang, F. Zhang and R. Babbush, OpenFermion: the electronic structure package for quantum computers, *Quantum Sci. Technol.* **2020**, *5*, 034014.
79. Quantum AI team and collaborators. (March 5, 2021). quantumlib/Cirq: Cirq, Version v0.10.0. Zenodo, http://doi.org/10.5281/zenodo.4586899.
80. M. W. Schmidt, K. K. Baldridge, J. A. Boatz, S. T. Elbert, M. S. Gordon, J. H. Jensen, S. Koseki, N. Matsunaga, K. A. Nguyen, S. Su, T. L. Windus, M. Dupuis, J. A. Montgomery, General atomic and molecular electronic structure system, *J. Comp. Chem.* **1993**, *14*, 1347–1363.
81. T. Yamada, S. Hirata, Singlet and triplet instability theorems, *J. Chem. Phys.* **2015**, *143*, 114112.
82. K. Sugisaki, S. Nakazawa, K. Toyota, K. Sato, D. Shiomi, T. Takui, Quantum chemistry on quantum computers: A method for preparation of multiconfigurational wave functions on quantum computers without performing post-Hartree–Fock calculations, *ACS Cent. Sci.* **2019**, *5*, 167–175.
83. K. Mitarai, M. Negoro, M. Kitagawa, K. Fujii, Quantum circuit learning, *Phys. Rev. A* **2018**, *98*, 032309.
84. R. M. Parrish, J. T. Iosue, A. Ozaeta, P. L. McMahon, A Jacobi diagonalization and Anderson acceleration algorithm for variational quantum algorithm parameter optimization, arXiv:1904.03206.
85. A. Kalemos, A. Mavridis, Electronic structure and bonding of ozone, *J. Chem. Phys.* **2008**, *129*, 054312.
86. M. Biczysko, L. A. Poveda, A. J. C. Varandas, Accurate MR-CI study of electronic ground-state N_2H_2 potential energy surface, *Chem. Phys. Lett.* **2006**, *424*, 46–53.
87. F. Plasser, H. Pašalić, M. H. Gerzabek, F. Libisch, R. Reiter, J. Burgdörfer, T. Müller, R. Shepard, H. Lischka, The multiradical character of one- and two-dimensional graphene nanoribbons, *Angew. Chem. Int. Ed.* **2013**, *52*, 2581–2584.